Chemosphere 111 (2014) 434–440

Contents lists available at ScienceDirect

Chemosphere

journal homepage: www.elsevier.com/locate/chemosphere

Kinetic modeling of antimony(V) adsorption–desorption and transport in soils

Hua Zhang [a,*], Lulu Li [b], Shiwei Zhou [a]

[a] Key Laboratory of Coastal Zone Environmental Processes and Ecological Remediation, Yantai Institute of Coastal Zone Research, Chinese Academy of Sciences, Yantai, Shandong, China
[b] College of Chemical and Environmental Engineering, Qingdao University, Qingdao, Shandong, China

HIGHLIGHTS

- Sb(V) sorption on soils were time-dependent and irreversible.
- Retention mechanisms were different for acidic red soil and calcareous soil.
- Sb(V) transport in soils dominated by non-equilibrium reactions.
- Kinetic reversible–irreversible MRM formulation well described experiment results.

GRAPHICAL ABSTRACT

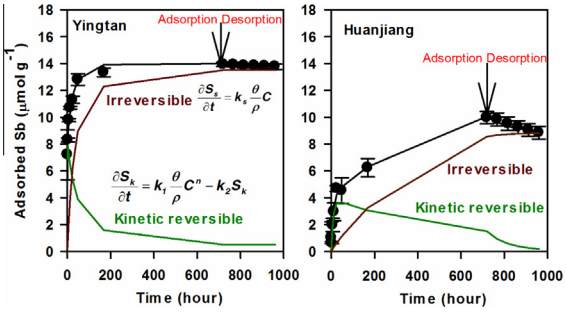

ARTICLE INFO

Article history:
Received 11 November 2013
Received in revised form 22 March 2014
Accepted 12 April 2014
Available online 16 May 2014

Handling Editor: X. Cao

Keywords:
Antimony
Soil
Adsorption–desorption
Transport
Mobility

ABSTRACT

Antimonate [Sb(V)] adsorption–desorption and transport in an acidic red soil (Yingtan) and a calcareous soil (Huanjiang) was investigated using kinetic batch and miscible displacement experiments. Different formulations of a multi-reaction model (MRM) were evaluated for their capabilities of describing the retention and transport mechanisms of Sb(V) in soils. The experimental results showed that adsorption of Sb(V) by two soils was kinetically controlled and largely irreversible. The Sb(V) adsorption capacity and kinetic rate of the acidic red soil was much higher than that of the calcareous soil. The asymmetrical breakthrough curves indicated the strong dominance of non-equilibrium retention of Sb(V). A four step sequential extraction procedure provided evidence that majority of applied Sb(V) was irreversibly retained. A formulation of MRM with two kinetic sorption sites (reversible and irreversible) successfully described Sb(V) adsorption–desorption data. The use of kinetic batch rate coefficients for predictions of breakthrough curves (BTCs) underestimated Sb(V) retention and overestimated its mobility. In an inverse mode with optimized rate coefficients, the MRM formulation was capable of simulating Sb(V) transport in soil columns.

1. Introduction

Elevated concentrations of antimony (Sb) in soils have caused increasing environmental concern because of its toxicity and suspected carcinogenicity for humans (Wilson et al. 2010; Belzile et al., 2011; Hockmann and Schulin, 2012). As the biggest Sb producer (approximately 90% of worldwide production), China has suffered serious Sb pollution in several regions, especially in the vicinity of metal mining and smelting sites such as Xikuangshan Sb mine, Diaojiang Se mine, and Yata Au mining areas. Soils in mining areas from southwestern China were extremely enriched in Sb with concentration up to 11 800 mg kg^{-1} (He, 2007; Okkenhaug et al., 2011; He et al., 2012). Human exposure to Sb through dietary and drinking water pathways near contaminated sites is a human

* Corresponding author. Tel.: +86 535 2109 180; fax: +86 535 2109 000.
E-mail address: hzhang@yic.ac.cn (H. Zhang).

http://dx.doi.org/10.1016/j.chemosphere.2014.04.054
0045-6535/

health concern (Okkenhaug et al., 2012). In addition, secondary contamination of groundwater and surface water by Sb leached from impacted soils pose further threat to ecological and human health (Willis et al., 2011).

Accurate assessment of environmental risk associated Sb contamination requires quantitative information on the bioavailability and mobility of Sb in soils. Geochemical property of Sb is in some respects similar to that of arsenic (As) because they have identical s^2p^3 outer orbital electron configuration but contrasting behavior of As and Sb has also been reported in literatures (Leuz et al., 2006; Lindsay et al., 2009; Fawcett and Jamieson, 2011; Beauchemin et al., 2012). The dominant forms of Sb in soil environment are antimonate [Sb(V)] under oxidized conditions and antimonite [Sb(III)] under reduced conditions (Leuz and Johnson, 2005; Leuz et al., 2006; Mitsunobu et al., 2006). It is reported that Sb(V) persists under anoxic conditions and very little Sb(III) is found downstream from stibnite mine because of the fast oxidation kinetics (Fawcett and Jamieson, 2011; Beauchemin et al., 2012). Adsorption–desorption on soil matrix and precipitation–dissolution of Sb minerals are believed to be the primary processes controlling the mobility of Sb in soils. The soil-solution distribution coefficients (K_d) of Sb measured for 110 Japanese agricultural soil samples ranged from 1 to 2100 L kg^{-1} and exhibited a decreasing trend with increasing pH and increasing phosphate concentration (Nakamaru et al., 2006). It appears that both Sb(III) and Sb(V) bind strongly to hydroxides of Fe, Al, and Mn and only weakly to clay minerals (Leuz and Johnson, 2005; Leuz et al., 2006). Recent extended X-ray absorption fine structure (EXAFS) analyses has demonstrated that Sb(V) form inner-sphere surface complex with Fe oxides, Al oxides, and clay minerals (Mitsunobu et al., 2010; Ilgen and Trainor, 2012). Surface complexation modeling conducted for Sb(III) and Sb(V) adsorption on iron rich red earth suggested the formation of bidentate mononuclear and binuclear complexes (Vithanage et al., 2013). Several studies have confirmed the strong influence of pH on Sb(V) sorption on Fe hydroxides with sorption maxima at low pH values and decreases after pH 7 (Tighe et al., 2005; Leuz et al., 2006; McComb et al., 2007). Sorption studies showed that large fractions of Sb sorbed on soils were non-exchangeable by ionic solution, suggesting the low mobility of Sb in soils (Hammel et al., 2000; Ettler et al., 2007). Sequential extraction results often suggested Sb association with Fe oxides in contaminated soils (Johnson et al., 2005; Ettler et al., 2010). EXAFS studies by Mitsunobu et al. (2006) and Scheinost et al. (2006) suggested that Sb in the soil is mainly associated with Fe(III) hydroxide and speciation of Sb in soil water showed that Sb was present exclusively as Sb(V), over a wide redox range. In addition, experiments showed that an equilibration time of 7 d is appropriate for Sb(V) sorption on goethite (Leuz et al., 2006). The kinetics of Sb(III) and Sb(V) adsorption on the Al-rich minerals is a relatively slow process extended to 720 h (Ilgen and Trainor, 2012), while kinetic rate of Sb(V) adsorption on bentonite was rapid initially and slowly approaching steady state after roughly 24 h (Xi et al., 2011). Spectroscopic study of Sb(V) adsorption/desorption to amorphous Fe oxide showed more rapid desorption under alkaline conditions (McComb et al., 2007). The kinetic batch experiments conducted by Martinez-Llado et al. (2011) have shown Sb(V) sorption on calcareous soils was relatively slow and follows a pseudo-second order rate equation.

There are significant knowledge gaps on the understanding of Sb transport in advective flow systems. Lysimeter experiments of Lewis et al. (2010) suggested Sb had relatively high mobility in the unsaturated shooting-range soil (coarse-grained sand, pH 4.8) as indicated by breakthrough occurring after 5–14 d and peak concentration reaching 124 μg L^{-1} after 29 d of infiltration. Column transport experiments by Martinez-Llado et al. (2011) showed that the breakthrough curves (BTCs) of Sb(V) through columns of calcareous soils were successfully described using equilibrium convection–dispersion equation (CDE) with very low distribution coefficients (K_d) between 0.45–1.55 L kg^{-1} and majority (82–89%) of applied Sb(V) was recovered in the effluent. The field lysimeter experiment of Hockmann and Schulin (2012) on Sb(V) contaminated (20 mg kg^{-1}) calcareous soil also showed early breakthrough of Sb(V) with maximum concentration (133 μg L^{-1}) reached after 5 weeks. In contrast Hou et al. (2013), investigated leaching and migration of Sb in three soils (Primosol, Isohumosol, and Ferrosol) of China using lysimeter experiments over a 5 month period and observed that the majority of the added Sb was retained in the top-soil layers with Sb in leachates less than 0.45 μg L^{-1}, indicating the low solubility of Sb in the soils. Moreover, studies on mining related contaminated sites often revealed that despite the high Sb concentration in soils, Sb was confined to the immediate vicinity of pollution sources and relatively little vertical movement was observed (Flynn et al., 2003; Wilson et al., 2004; He, 2007; Lindsay et al., 2011). For example, Sb was confined to the upper 10 cm in soil profile near a lead smelter after long history of ore processing (Ettler et al., 2010). This wide discrepancy on Sb mobility warrant detailed investigation on Sb transport in different types of soils and varying geochemical settings. Furthermore, although numerical models incorporating kinetic reactions and transport processes have been proven as a valuable tool for predicting fate and behavior of metals and metalloids (Zhang and Selim, 2005, 2006), their capabilities in simulating the retention of transport of Sb in soils has not been evaluated.

The main goal of this study is to (i) quantify the time-dependent adsorption–desorption and transport behavior of Sb(V) in two soils with contrasting properties (an acidic red soil and a calcareous soil) using batch and column experiments; and (ii) test the applicability of different formulations of MRM in simulating non-equilibrium sorption and transport of Sb(V) in soils. This information is important for evaluating the environmental risks associated with Sb release at contaminated sites.

2. Material and methods

2.1. Soils

Uncontaminated soil samples of an acidic red soil (Yingtan) and a calcareous soil (Huanjiang) were collected from Yingtan Red Soil Ecological Experiment Station and Huanjiang Observation and Research Station for Karst Ecosystems of the Chinese Academy of Sciences (CAS), respectively. Both samples were obtained from surface layer (0–20 cm), air-dried, and sieved through 2 mm screen before use. The basic chemical and physical properties of the two

Table 1
Selected physical and chemical properties of the studied soils.

Soil	Yingtan	Huanjiang
Chinese soil taxonomy	Hap-udic ferrisols	Cab-udic cambisols
FAO classification	Haplic acrisol	Chromic cambisol
pH	4.8	7.4
TOC[a] (g kg^{-1})	2.1	25
CEC[b] (cmol kg^{-1})	16	25
Total Fe (g kg^{-1})	26	52
Total Al (g kg^{-1})	13	22
Oxalate Fe (g kg^{-1})	0.12	0.19
Oxalate Al (g kg^{-1})	0.46	0.53
Sand[c] (%)	31	33
Silt (%)	54	49
Clay (%)	14	16

[a] TOC = total organic carbon.
[b] CEC = cation exchange capacity.
[c] Grain size distribution: sand (2.00–0.05 mm), silt (0.05–0.002 mm), and clay (<0.002 mm).

soils are given in Table 1 and detailed description of analytical methods can be found in supplementary content. Both soils have high iron and aluminum contents and their particle size distributions are similar.

2.2. Adsorption–desorption experiments

Kinetic batch experiments were conducted to determine Sb(V) adsorption–desorption on the soils at constant room temperature of 25 °C under oxidized conditions (Zhang and Selim, 2005). Three initial concentrations C_o (0.02, 0.16 and 1.48 mM) of $KSb(OH)_6$ were prepared in 0.01 M $KClO_4$ background solution to maintain constant ionic strength. Experiments were initiated by mixing 3.00 g of air dry soil with 30 mL of Sb(V) solution in a 50-mL Teflon tube. The mixtures were shaken at 150 rpm on a reciprocal shaker and subsequently centrifuged for 10 min at 4000 rpm at reaction times of 0.5, 2, 6, 12, 24, 48, 168, and 720 h. A 1-mL aliquot was sampled from the supernatant and subsequently diluted to 10 mL. After sampling, the slurry was agitated using a vortex mixer and returned to the shaker. The concentrations of total Sb were analyzed using inductively coupled plasma mass spectrometry (ICP-MS, ELAN DRC II, Perkin Elmer SCIEX, USA). Amount of Sb(V) adsorption was calculated from the difference between concentrations of the supernatant and that of the initial solutions. For each input concentration C_o, the tests were performed in triplicates and the mean and standard error (SE) of the amount of Sb(V) adsorbed is reported.

The extent of release or desorption of Sb(V) was quantified using the same batch system immediately after the last adsorption step (720 h). Each desorption step was carried out by decanting supernatant after centrifugation, replacing with 25 mL 0.01 M $KClO_4$ background solution, and shaking for 48 h. This desorption step was iterated five times with a total desorption time of 240 h. The fraction of Sb(V) desorbed from the soils were calculated based on the change in concentration in solution (before and after desorption). Moreover, during adsorption as well as desorption experiments, pH of the supernatant was measured and reported in supplementary content. Residual soils from adsorption–desorption experiments were stored at 4 °C before sequential chemical extraction.

2.3. Miscible displacement experiments

The transport of Sb(V) in soils was investigated using the saturated miscible displacement technique (Zhang and Selim, 2006). Acrylic columns (8.5-cm in length and of 2.5-cm i.d.) were uniformly packed with air-dried soil and were slowly water-saturated with a background solution of 0.01 M $KClO_4$ at a low Darcy flux until effluent pH reached steady state (4.54 for Yingtan soil and 7.36 for Huanjiang soil). Input solution of 0.15 mM Sb(V) in 0.01 M $KClO_4$ was subsequently introduced to each soil column at constant flow rate with a peristaltic pump (BT 102S, Baoding Longer Precision Pump Co., Ltd., Hebei, China). It was followed by a leaching or desorption pulse consists of pumping the background solution. Effluent samples were collected from the outlet of the column by an automatic effluent collector (CBS-A, Shanghai Huxi Analysis Instrument Factory Co., Ltd., Shanghai) at 1 h time interval. Soil columns were sectioned at 2 cm interval after experiments and stored at 4 °C before sequential chemical extraction.

2.4. Sequential extraction

Sequential extraction procedure is employed to understand the chemical binding of Sb in soil. A simplified four step chemical extraction procedure as described by Okkenhaug et al. (2011) was carried out on freeze dried soil samples from kinetic batch and column experiments.[11] The four fractions are referred to here as non-specifically sorbed [extraction by 0.05 M $(NH_4)_2SO_4$], specifically sorbed [0.05 M $(NH_4)H_2PO_4$), Fe and Al oxides bound (0.2 M NH_4-oxalate buffer and 0.1 M ascorbic acid; pH 3.25), and residual (concentrated HF, HNO_3, and $HClO_4$ in a ratio of 5:2:1). The first two phases were measured by mixing 1 g soil with 25 mL of the extractant solution, shaking for 16 h, and centrifuging. The oxalate extraction step was carried out for 30 min in a water basin at 96 ± 3 °C in the light. Total acid digestion of soil samples was carried out in a closed microwave digestion device (190 °C, 15 min) with 0.2 g sample and 6 mL concentrated acid.

2.5. Multi-reaction transport model

The multi-reaction model (MRM) developed by Selim et al. (1989) is utilized for describing the kinetic adsorption–desorption of Sb(V) in the soils. Specifically, the model assumes that a fraction of the total sorption sites is kinetic in nature whereas the remaining fractions interact rapidly or instantaneously with solute in the soil solution. The model accounts for reversible as well as irreversible sorption of the concurrent and consecutive type. The model used in this analysis can be presented in the following formulations:

$$\text{Equilibrium } S_e = K_e \frac{\theta}{\rho} C^n \tag{1}$$

$$\text{Reversible Kinetic } \frac{\partial S_k}{\partial t} = k_1 \frac{\theta}{\rho} C^n - k_2 S_k \tag{2}$$

$$\text{Irreversible } \frac{\partial S_i}{\partial t} = k_3 S_k \tag{3}$$

$$\text{Concurrent irreversible } \frac{\partial S_s}{\partial t} = k_s \frac{\theta}{\rho} C \tag{4}$$

Here C is the concentration in solution (μmol L^{-1}), S_e is the amount retained on equilibrium sites (μmol g^{-1}), S_k is the amount retained on kinetic type sites (μmol g^{-1}), S_i is the amount retained irreversibly by consecutive reaction (μmol g^{-1}), S_s is the amount retained irreversibly by concurrent type of reaction (μmol g^{-1}), K_e is a dimensionless equilibrium constant, k_1 and k_2 (h^{-1}) are the forward and backward reaction rate associated with kinetic sites, respectively, k_3 (h^{-1}) is the irreversible rate coefficient associate with the kinetic sites, n is the dimensionless reaction order, θ is the soil water content ($cm^3\ cm^{-3}$), ρ is the soil bulk density (g cm^{-3}), and t is the reaction time (h). The total amount of solute retention on soil is:

$$S = S_e + S_k + S_i + S_S \tag{5}$$

To simulate the reactive transport of Sb(V) through soils, the MRM adsorption–desorption formulations are incorporated into the steady state advection–dispersion equation (ADE) in the form of (Selim et al., 1989):

$$\frac{\partial C}{\partial t} + \frac{\rho}{\theta}\frac{\partial S}{\partial t} = \frac{\partial}{\partial x}\left(D\frac{\partial C}{\partial x}\right) - v\frac{\partial C}{\partial x} \tag{6}$$

where x is distance (cm), D is hydrodynamic dispersion coefficient ($cm^2\ h^{-1}$), and v is pore water velocity (cm h^{-1}).

Statistical criteria used for estimating the goodness-of-fit of the models to the data were the coefficients of determination (r^2) and the root mean square error (RMSE)

$$\text{RMSE} = \sqrt{\frac{\sum (C_{obs} - C_{mod})^2}{n_{obs} - n_{par}}} \tag{7}$$

where C_{obs} is the observed Sb(V) concentration at certain time t, C_{mod} is the simulated Sb(V) concentration at time t, n_{obs} is the number of measurements, and n_{par} is the number of fitted parameters.

3. Results and discussion

3.1. Adsorption isotherms

Adsorption isotherms describing the distribution of Sb(V) between aqueous (C) and sorbed phases (S) are presented in Fig. 1. The Freundlich equation is utilized to describe such adsorption isotherms.

$$S = K_F C^b \quad (8)$$

where K_F is the Freundlich distribution or partition coefficient, and b is the dimensionless reaction order commonly less than one. The Sb(V) isotherms of Fig. 1 clearly exhibit nonlinear adsorption behavior, which is characterized by the low values of the Freundlich nonlinear reaction order for Yingtan ($b = 0.413 \pm 0.035$) and Huanjiang ($b = 0.676 \pm 0.045$) soil. The low values of b illustrate the dependence of the sorption process on concentration where sorption by the highest energy sites takes place preferentially at the lowest solution concentration. A comparison between the Freundlich parameters demonstrated that Sb(V) adsorption of the acidic Yingtan soil was greater and more nonlinear than that of the calcareous Huanjiang soil. Several studies have emphasized the importance of metal oxides as major components determining the soils' sorption capacity for Sb (Tighe et al., 2005; Martinez-Llado et al., 2011; Vithanage et al., 2013). In our experiments, both soils had relatively high iron and aluminum contents. However, difference between pH of Yingtan soil (4.8) and calcareous Huanjiang soil (7.4) can be used to partially explain its higher adsorption capacity. This is consistent with previous studies showing that Sb(V) adsorption decrease with increasing pH in the range of 3–7 (Tighe et al., 2005; Leuz et al., 2006; Martinez-Llado et al., 2011; Vithanage et al., 2013).

3.2. Kinetic adsorption–desorption

The time-dependent adsorption–desorption processes of Sb(V) were illustrated for the various initial concentrations by the two soils (Fig. 2). The rapid retention at low solution concentrations is consistent with the nonlinear adsorption isotherms, indicating preferential sorption on high energy sites. At high initial concentrations ($C_o = 1.48$ mM), the kinetic rate of Sb(V) adsorption on Yingtan soil was much faster than Huanjiang soil, reflecting different soil properties. Relatively few studies have investigated the adsorption–desorption kinetics of Sb. Studies on pure mineral phases often revealed that Sb adsorption was initially fast followed by a slow kinetic process extended for several days (Leuz and Johnson, 2005; Leuz et al., 2006; McComb et al., 2007; Xi et al., 2011; Ilgen and Trainor, 2012). The study of Sb(V) sorption on Japanese soils conducted by Nakamaru et al. (2006) concluded that 7-d reaction time was sufficient to achieve equilibrium of Sb sorption. Martinez-Llado et al. (2011) studied Sb(V) sorption on calcareous soils and found the sorption kinetics was relatively slow with equilibrium reached after days. Our experiment results also revealed that the kinetic rate of Sb(V) sorption can vary in a wide range depending on soil surface characteristics and solution concentration. The time-dependent sorption behavior has to be considered in modeling the fate and transport of Sb in soils.

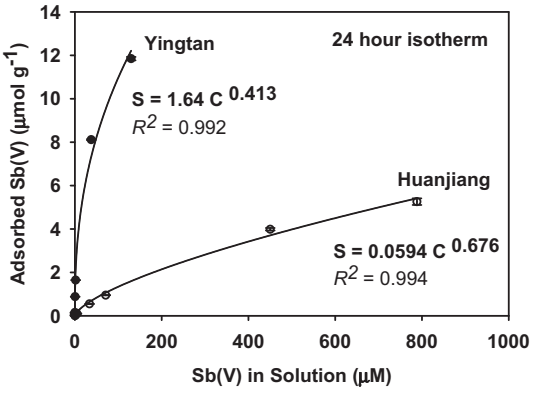

Fig. 1. Isotherms of antimony(V) adsorption on Yingtan and Huanjiang soils. The lines depict results of curve-fitting with Freundlich equation.

Desorption followed immediately after adsorption demonstrated that only small proportions were released by background solution, indicating high sorption affinity between Sb(V) and the soil matrix. Overall, Sb adsorption on soils is not reversible. The acidic red soil (Yingtan) has surprisingly high binding strength, whereas only 0.2–1.9% of the sorbed Sb(V) was released after five desorption steps. In comparison, 12–14% of sorbed Sb(V) was released back into solution from Huanjiang soils, indicating weaker affinity of Sb(V) on surface of this calcareous soil. It should be noted that the amount of desorption were relatively stable in respect to initial concentration, which span three order of magnitudes. The ATR-IR spectroscopic study of McComb et al. (2007) showed that desorption of Sb(V) from iron oxide is more rapid at higher pH. Therefore, the contrasting soil pH might be a possible explanation to the difference in desorption kinetics of the two soils.

Sequential chemical extraction results in Fig. 2 showed that the sulfate extractable Sb fraction varied between 0.9–3.0% and 3.4–6.4% for Yingtan and Huanjiang soils, respectively. This non-specifically bound and readily leachable fraction constituted only a small fraction of the Sb sorbed by soils, which is consistent with the slight desorption observed in the kinetic batch experiment. It is often believed that phosphate has chemical properties similar to those of antimonate and thus can replace Sb(V) on adsorption sites (Nakamaru and Sekine, 2008; Biver et al., 2011). However, the extraction results showed that only 1.9–3.4% and 8.0–8.6% of the total amounts of Sb sorbed were replaced by phosphate for Yingtan and Huanjiang soils, respectively. This is consistent with the findings from previous chemical extraction studies conducted on contaminated soils (Ettler et al., 2007; Okkenhaug et al. 2011). Oxalate extracted Sb constituted 53–55% and 38–43% of the total amount of Sb sorbed by Yingtan and Huanjiang soils, respectively. Ammonium oxalate extractant was used to break up the strong linkage between Fe/Al oxide and Sb(V). This fraction of Sb is strongly bound to Fe/Al oxides as surface complexation or precipitation and unlikely to be mobilized unless under extremely reduced conditions (Okkenhaug et al. 2011). Beside phosphate-extractable and oxalate extracted phase, other recalcitrant components of Sb made up 33–39% and 27–40% of the total amount of Sb sorbed by Yingtan and Huanjiang soils, respectively, as determined by digestion with strong acid at high temperature. Similar results have been observed on Sb contaminated soils near mining sites, which showed extractable Sb was only a minor fraction of the total Sb retained in soils and the majority of Sb was in the oxide-bounded or residue forms (King, 1988; Wilson et al., 2004; He, 2007; Ettler et al., 2010; Okkenhaug et al., 2011).

3.3. Reactive transport

The breakthrough curves (BTCs) from column experiments illustrate the extensive retention and low mobility of Sb(V) in the two soils. Complete breakthrough, i.e. 100% recovery of that applied, was not observed in any of the soil columns following extended Sb(V) input pulses (Fig. 3). All measured Sb(V) BTCs exhibited extensive asymmetry as illustrated by the difference in the shape of the effluent side from the leaching or desorption side. The breakthrough of Sb(V) from Yingtan column showed an extremely long period of retardation (>150 pore volumes). After

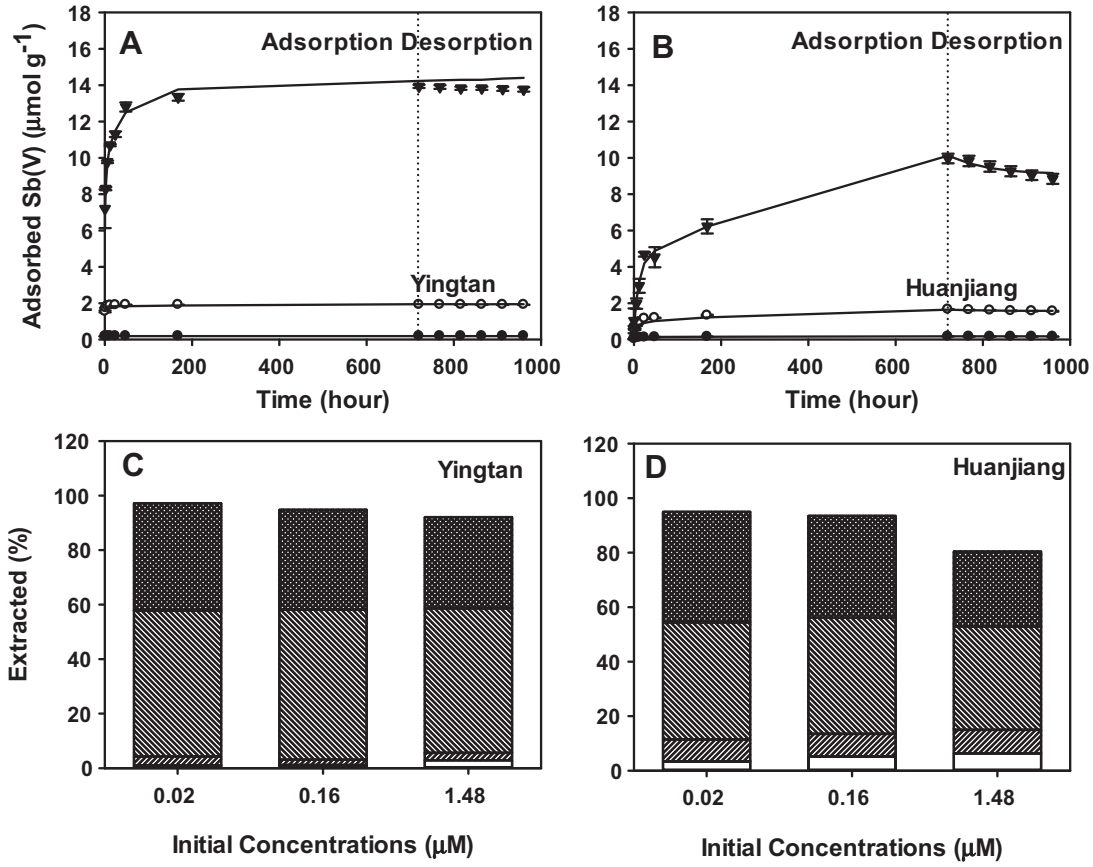

Fig. 2. Adsorption–desorption kinetics and retention phases of antimony(V) in Yingtan and Huanjiang soils. (A and B): antimony(V) concentration in solution as a function of reaction time during adsorption–desorption on Yingtan (A) and Huanjiang (B) soils. Symbols are for different initial concentrations (C_o). Lines are multi-reaction model (MRM) simulations using parameters obtained from nonlinear optimization. Broken lines indicate desorption start times. (C and D): Retention phases of antimony in Yingtan (C) and Huanjiang (D) soils determined from sequential extraction. Different pattern illustrate antimony distribution among the following pools (from bottom to top): P1 = extracted with 0.05 M $(NH_4)_2SO_4$, P2 = extracted with 1 M NaH_2PO_4, P3 = extracted with 0.2 M ammonium oxalate, and P4 = digested with mixed acids of HNO_3, HF, and $HClO_4$.

applying approximately 350 pore volumes of Sb(V) solution, the peak Sb(V) concentration in the effluent was only about 10% of the applied concentration. The shape of BTCs from calcareous Huanjiang soil was dramatically different from acidic Yingtan soil, reflecting the intrinsic difference in soil properties. The transport of Sb(V) in Huanjiang soil showed a diffuse BTC front, characterized by gradual increase of Sb concentration to approximately 50% of the input concentration after 95 pore volumes. In addition, the excessive tailing exhibited by column BTCs demonstrated a continued slow desorption (release) of Sb(V) from soils. Diffusive fronts, strong retardation, and extensive tailing or slow release during leaching are features of non-equilibrium transport. The extent of retention given by column experiments agrees with the relative degree of adsorption as measured from the batch isotherms (see Fig. 1), i.e., Yingtan soil with high adsorption capacity exhibited a substantially higher retardation than Huanjiang soil. The observed non-equilibrium transport of Sb(V) in soils agrees with the highly nonlinear and kinetic adsorption behavior observed in our batch experiments (see Fig. 2). In addition, the BTC from calcareous Huanjiang soil had similar shape of the BTCs from column experiments of Martinez-Llado et al. (2011), in which calcareous soils with pH 7.0–7.8 were used.

Sb fractions retained by soil at different depth after column experiments were determined using sequential chemical extraction (Fig. 3). The results showed that a dominant fraction of Sb(V) input was irreversibly retained in soil columns and was not released by background solution. Distribution of Sb in the four retention phases was in good agreement with the extraction results on soils from kinetic batch experiments, i.e., the majority of Sb was retained in the oxide-bounded and residual phases and only a small fraction was exchangeable by sulfate and phosphate solutions. The vertical distribution of Sb(V) showed that kinetic retention on soil is the dominant mechanism controlling its transport with flowing water.

3.4. Multi-reaction modeling

In heterogeneous soil systems, time-dependent retention/release of metals and metalloids may be a result of several different mechanisms including (1) heterogeneity of sorption sites with varying degrees of affinities, (2) slow diffusion to/from sites within the soil matrix, and (3) kinetic precipitation/dissolution at the mineral surface (Zhang and Selim, 2005, 2006). Therefore, we rigorously tested different formulations of the MRM representing different reactions from which one can deduce retention mechanisms. Detailed description of the modeling process is provided in supplementary content. We found that the use of a 3-parameter model where retention is accounted for by a reversible (S_k) and a concurrent irreversible (S_s) phases provided best goodness-of-fit for describing Sb(V) adsorption–desorption kinetics. Our results was similar to that of Zhang and Selim (2006), whereas a 3 parameter formulation with kinetic reversible and irreversible retention phases was shown to be superior than other MRM formulations for describing arsenate adsorption–desorption in soils.

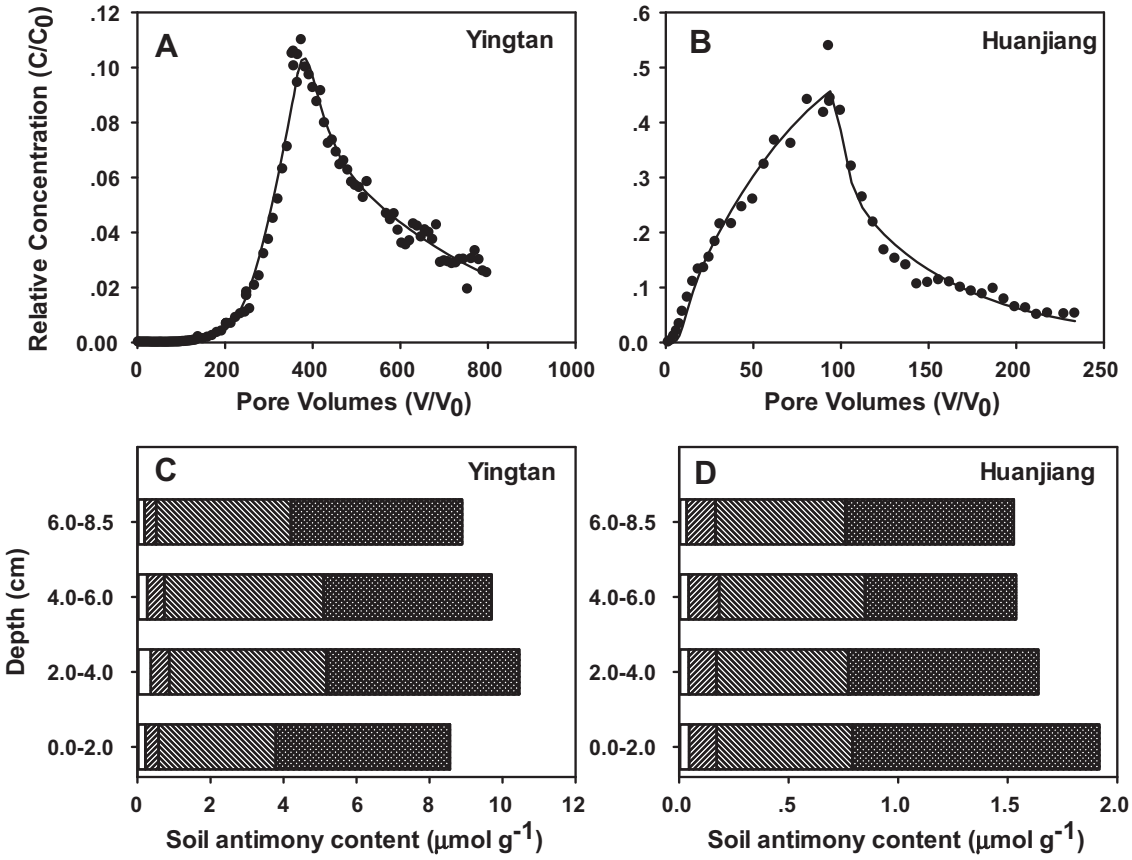

Fig. 3. Breakthrough curves of antimony from columns and vertical distribution of antimony among retention phase in Yingtan and Huanjiang soils. (A and B): Breakthrough curves obtained from column experiments of Sb(V) reactive transport in Yingtan (A) and Huanjiang (B) soils. Symbols are experiment observations. Lines are multi-reaction model (MRM) simulations using parameters obtained from nonlinear optimization. (C and D): Vertical distribution of antimony among retention phases Yingtan (C) and Huanjiang (D) soils as determined from sequential extraction. Different pattern illustrate antimony distribution among the following pools (from bottom to top): P1 = extracted with 0.05 M $(NH_4)_2SO_4$, P2 = extracted with 1 M NaH_2PO_4, P3 = extracted with 0.2 M ammonium oxalate, and P4 = digested with mixed acids of HNO_3, HF, and $HClO_4$.

Our simulation results showed that adsorption–desorption rate coefficients obtained from column BTCs were much larger than those obtained from kinetic batch experiments, which indicated higher Sb(V) sorption in miscible displacement experiments than batch experiments. It was suggested that the following reasons should be accounted: (1) differences in pore-water velocity and hence the difference between sorption time in batch experiment and hydrologic residence time in displacement experiment; (2) low soil/solution ratio used in batch experiments; (3) reactant was added in one spike for batch study compared to continuous addition in column experiments; and (4) potential buildup of reaction products in closed batch systems (Zhang and Selim, 2006). In addition, the increased spatial heterogeneity in displacement experiment can result in the change of macroscopic adsorptive kinetics (Zhang et al., 2013).

4. Conclusion

Evaluating environmental risk of Sb contamination in soil have to include the kinetic adsorption–desorption and reactive transport processes. In this study, the batch and column experiment results revealed the dominance of non-equilibrium and irreversible retention of Sb(V) by soils. It is demonstrated that Sb released into environment can persist for very long time and the slow desorption/release of Sb may pose a threat to surface water and groundwater. A multiple reaction model was successfully utilized in describing retention (adsorption) and subsequent release or leaching (desorption) observations in both kinetic batch and column experiments over a wide range of Sb concentrations. A simple MRM formulation with two kinetic sorption sites (reversible and irreversible) was found to be sufficient for simulating Sb(V) retention and transport. The modeling data from this study can be used for pre-screening the risk of Sb release and movement at heavily contaminated sites.

Acknowledgments

The authors would like to thank Dr. Chengli Qu and Xueli Wu for chemical analysis. This work was financially supported by National Natural Science Foundation of China (41271506, 41230858) and the Key Research Program of Chinese Academy of Sciences (KZZD-EW-14). Dr. Hua Zhang was financially supported by the Recruitment Program of Global Young Experts (1000Plan).

Appendix A. Supplementary material

Supplementary data associated with this article can be found, in the online version, at http://dx.doi.org/10.1016/j.chemosphere.2014.04.054.

References

Beauchemin, S., Kwong, Y.T.J., Desbarats, A.J., MacKinnon, T., Percival, J.B., Parsons, M.B., Pandya, K., 2012. Downstream changes in antimony and arsenic speciation in sediments at a mesothermal gold deposit in British Columbia. Can. Appl. Geochem. 27, 1953–1965.

Belzile, N., Chen, Y.-W., Filella, M., 2011. Human exposure to antimony: i. sources and intake. Crit. Rev. Environ. Sci. Technol. 41, 1309–1373.

Biver, M., Krachler, M., Shotyk, W., 2011. The desorption of antimony(v) from sediments, hydrous oxides, and clay minerals by carbonate, phosphate, sulfate, nitrate, and chloride. J. Environ. Qual. 40, 1143–1152.
Ettler, V., Mihaljevic, M., Sebek, O., Nechutny, Z., 2007. Antimony availability in highly polluted soils and sediments – a comparison of single extractions. Chemosphere 68, 455–463.
Ettler, V., Tejnecky, V., Mihaljevic, M., Sebek, O., Zuna, M., Vanek, A., 2010. Antimony mobility in lead smelter-polluted soils. Geoderma 155, 409–418.
Fawcett, S.E., Jamieson, H.E., 2011. The distinction between ore processing and post-depositional transformation on the speciation of arsenic and antimony in mine waste and sediment. Chem. Geol. 283, 109–118.
Flynn, H.C., Meharg, A.A., Bowyer, P.K., Paton, G.I., 2003. Antimony bioavailability in mine soils. Environ. Pollut. 124, 93–100.
Hammel, W., Debus, R., Steubing, L., 2000. Mobility of antimony in soil and its availability to plants. Chemosphere 41, 1791–1798.
He, M., 2007. Distribution and phytoavailability of antimony at an antimony mining and smelting area, Hunan. China. Environ. Geochem. Health 29, 209–219.
He, M., Wang, X., Wu, F., Fu, Z., 2012. Antimony pollution in China. Sci. Total Environ. 421–422, 41–50.
Hockmann, K., Schulin, R., 2012. Leaching of antimony from contaminated soils. In: Selim, H.M. (Ed.), Competitive Sorption and Transport of Heavy Metals in Soils and Geological Media. CRC Press, Boca Raton, FL, pp. 119–145.
Hou, H., Yao, N., Li, J.N., Wei, Y., Zhao, L., Zhang, J., Li, F.S., 2013. Migration and leaching risk of extraneous antimony in three representative soils of China: lysimeter and batch experiments. Chemosphere 93, 1980–1988.
Ilgen, A.G., Trainor, T.P., 2012. Sb(III) and Sb(V) sorption onto Al-rich phases: hydrous al oxide and the clay minerals kaolinite KGa-1b and oxidized and reduced nontronite NAu-1. Environ. Sci. Technol. 46, 843–851.
Johnson, C.A., Moench, H., Wersin, P., Kugler, P., Wenger, C., 2005. Solubility of antimony and other elements in samples taken from shooting ranges. J. Environ. Qual. 34, 248–254.
King, L.D., 1988. Retention of metals by several soils of the southeastern United States. J. Environ. Qual. 17, 239–246.
Leuz, A.-K., Monch, H., Johnson, C.A., 2006. Sorption of Sb(III) and Sb(V) to goethite: influence on Sb(III) oxidation and mobilization. Environ. Sci. Technol. 40, 7277–7282.
Leuz, A.K., Johnson, C.A.R., 2005. Oxidation of Sb(III) to Sb(V) by O-2 and H_2O_2 in aqueous solutions. Geochim. Cosmochim. Acta 69, 1165–1172.
Lewis, J., Sjostrom, J., Skyllberg, U., Hagglund, L., 2010. Distribution, chemical speciation, and mobility of lead and antimony originating from small arms ammunition in a coarse-grained unsaturated surface sand. J. Environ. Qual. 39, 863–870.
Lindsay, M.B.J., Blowes, D.W., Ptacek, C.J., Condon, P.D., 2011. Transport and attenuation of metal(loid)s in mine tailings amended with organic carbon: column experiments. J. Contam. Hydrol. 125, 26–38.
Lindsay, M.B.J., Condon, P.D., Jambor, J.L., Lear, K.G., Blowes, D.W., Ptacek, C.J., 2009. Mineralogical, geochemical, and microbial investigation of a sulfide-rich tailings deposit characterized by neutral drainage. Appl. Geochem. 24, 2212–2221.
Martinez-Llado, X., Valderrama, C., Rovira, M., Marti, V., Gimenez, J., de Pablo, J., 2011. Sorption and mobility of Sb(V) in calcareous soils of Catalonia (NE Spain): batch and column experiments. Geoderma 160, 468–476.
McComb, K.A., Craw, D., McQuillan, A.J., 2007. ATR-IR spectroscopic study of antimonate adsorption to iron oxide. Langmuir 23, 12125–12130.
Mitsunobu, S., Harada, T., Takahashi, Y., 2006. Comparison of antimony behavior with that of arsenic under various soil redox conditions. Environ. Sci. Technol. 40, 7270–7276.
Mitsunobu, S., Takahashi, Y., Terada, Y., Sakata, M., 2010. Antimony(V) incorporation into synthetic ferrihydrite, goethite, and natural iron oxyhydroxides. Environ. Sci. Technol. 44, 3712–3718.
Nakamaru, Y.M., Sekine, K., 2008. Sorption behavior of selenium and antimony in soils as a function of phosphate ion concentration. Soil Sci. Plant Nutr. 54, 332–341.
Nakamaru, Y., Tagami, K., Uchida, S., 2006. Antimony mobility in Japanese agricultural soils and the factors affecting antimony sorption behavior. Environ. Pollut. 141, 321–326.
Okkenhaug, G., Zhu, Y.-G., He, J., Li, X., Luo, L., Mulder, J., 2012. Antimony (Sb) and arsenic (As) in Sb mining impacted paddy soil from Xikuangshan, China: differences in mechanisms controlling soil sequestration and uptake in rice. Environ. Sci. Technol. 46, 3155–3162.
Okkenhaug, G., Zhu, Y.-G., Luo, L., Lei, M., Li, X., Mulder, J., 2011. Distribution, speciation and availability of antimony (Sb) in soils and terrestrial plants from an active Sb mining area. Environ. Pollut. 159, 2427–2434.
Scheinost, A.C., Rossberg, A., Vantelon, D., Xifra, I., Kretzschmar, R., Leuz, A.-K., Funke, H., Johnson, C.A., 2006. Quantitative antimony speciation in shooting-range soils by EXAFS spectroscopy. Geochim. Cosmochim. Acta 70, 3299–3312.
Selim, H.M., Amacher, M.C., Iskandar, I.K., 1989. Modeling the transport of chromium(vi) in soil columns. Soil Sci. Soc. Am. J. 53, 996–1004.
Tighe, M., Lockwood, P., Wilson, S., 2005. Adsorption of antimony(v) by floodplain soils, amorphous iron(III) hydroxide and humic acid. J. Environ. Monit. 7, 1177–1185.
Vithanage, M., Rajapaksha, A.U., Dou, X., Bolan, N.S., Yang, J.E., Ok, Y.S., 2013. Surface complexation modeling and spectroscopic evidence of antimony adsorption on iron-oxide-rich red earth soils. J. Colloid Interface Sci. 406, 217–224.
Willis, S.S., Haque, S.E., Johannesson, K.H., 2011. Arsenic and antimony in groundwater flow systems: a comparative study. Aquat. Geochem. 17, 775–807.
Wilson, N.J., Craw, D., Hunter, K., 2004. Antimony distribution and environmental mobility at an historic antimony smelter site, New Zealand. Environ. Pollut. 129, 257–266.
Wilson, S.C., Lockwood, P.V., Ashley, P.M., Tighe, M., 2010. The chemistry and behaviour of antimony in the soil environment with comparisons to arsenic: a critical review. Environ. Pollut. 158, 1169–1181.
Xi, J., He, M., Lin, C., 2011. Adsorption of antimony(III) and antimony(V) on bentonite: kinetics, thermodynamics and anion competition. Microchem. J. 97, 85–91.
Zhang, H., Selim, H.M., 2005. Kinetics of arsenate adsorption–desorption in soils. Environ. Sci. Technol. 39, 6101–6108.
Zhang, H., Selim, H.M., 2006. Modeling the transport and retention of arsenic (V) in soils. Soil Sci. Soc. Am. J. 70, 1677–1687.
Zhang, X., Jiang, B., Zhang, X., 2013. Reliability of the multiple-rate adsorptive model for simulating adsorptive solute transport in soil demonstrated by pore-scale simulations. Transp. Porous Media 98, 725–741.